Design and synthesis of a novel, orally active, brain penetrant, tri-substituted thiophene based JNK inhibitor

Simeon Bowers [a,*], Anh P. Truong [a,*], R. Jeffrey Neitz [a], Martin Neitzel [a], Gary D. Probst [a], Roy K. Hom [a], Brian Peterson [a], Robert A. Galemmo Jr. [a], Andrei W. Konradi [a], Hing L. Sham [a], Gergley Tóth [b], Hu Pan [b], Nanhua Yao [b], Dean R. Artis [b], Elizabeth F. Brigham [c], Kevin P. Quinn [d], John-Michael Sauer [d], Kyle Powell [e], Lany Ruslim [e], Zhao Ren [e], Frédérique Bard [e], Ted A. Yednock [a,b,c,d,e], Irene Griswold-Prenner [e]

[a] Department of Chemical Sciences, Elan Pharmaceuticals, 180 Oyster Point Boulevard, South San Francisco, CA 94080, United States
[b] Department of Molecular Design, Elan Pharmaceuticals, 180 Oyster Point Boulevard, South San Francisco, CA 94080, United States
[c] Department of Pharmacology, Elan Pharmaceuticals, 800 Gateway Boulevard, South San Francisco, CA 94080, United States
[d] Department of Lead Finding, Drug Disposition, and Safety Evaluation, Elan Pharmaceuticals, 800 Gateway Boulevard, South San Francisco, CA 94080, United States
[e] Department of Biology, Elan Pharmaceuticals, 1000 Gateway Boulevard, South San Francisco, CA 94080, United States

ABSTRACT

The SAR of a series of tri-substituted thiophene JNK3 inhibitors is described. By optimizing both the N-aryl acetamide region of the inhibitor and the 4-position of the thiophene we obtained single digit nanomolar compounds, such as 47, which demonstrated an in vivo effect on JNK activity when dosed orally in our kainic acid mouse model as measured by phospho-c-jun reduction.

© 2011 Elsevier Ltd. All rights reserved.

The c-Jun N-terminal kinases (JNKs) are serine/threonine protein kinases in the mitogen-activated protein kinase (MAPK) family.[1] The JNKs regulate signal transduction in response to stress stimuli such as UV light, reactive oxygen species, cytokines, hypoxia and protein misfolding.[2] Three isoforms of JNK have been identified: JNK1, JNK2 and JNK3.[3] JNK1 and JNK2 are ubiquitously expressed while JNK3 is localized primarily in the brain.[4] JNK1 is suggested to play a role in metabolic disorders such as type-2 diabetes[1] while JNK2 is involved in the pathology of autoimmune diseases such as rheumatoid arthritis and asthma as well as vascular diseases and atherosclerosis.[1] JNK3 has been implicated in playing important roles in models of neurodegeneration such as the synaptic loss associated with Alzheimer's disease, mediation of neurotoxicity in Parkinson's disease as well as involvement in Huntington's disease, and cerebral ischemia.[5] JNK3 knockout mice are viable and when treated with the neuroexcitotoxin kainic acid, they show decreased neuronal death and seizure activity.[6a] In a separate study, JNK3 knockout mice showed reduced downstream c-Jun phosphorylation and reduced brain injury after cerebral ischemia-hypoxia

compared to wild-type animals.[6b] Taken together, these data imply that inhibition of JNK3 may be neuroprotective.

For a JNK3 inhibitor to demonstrate in vivo neuroprotection it must be brain penetrant and have high kinase selectivity to avoid potential toxicity. While there are reports of selective JNK3 inhibitors,[7] we focused on JNK inhibitors with selectivity over the closely related MAP kinases p38α and ERK2.[1h] Previously, we have reported a class of thiophene based JNK inhibitors such as compound 1 (Fig. 1) which displayed favorable permeability, low P-gp efflux and selectivity for JNK over p38α and ERK2.[8] Reported in this Letter are our efforts to improve the JNK3 potency of this class of compounds while retaining their good selectivity and pharmacokinetic properties.
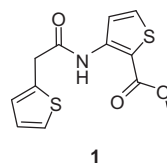
JNK3 IC$_{50}$ = 2.2 μM
JNK2 IC$_{50}$ = 23 μM
JNK1 IC$_{50}$ = 1.6 μM
p38α IC$_{50}$ > 50 μM
ERK2 IC$_{50}$ > 50 μM
Hank's Buffered Salt Solution solubility = 72 μM
MDR MDCK A>B = 144 nm/sec
P-gp efflux = 0.93

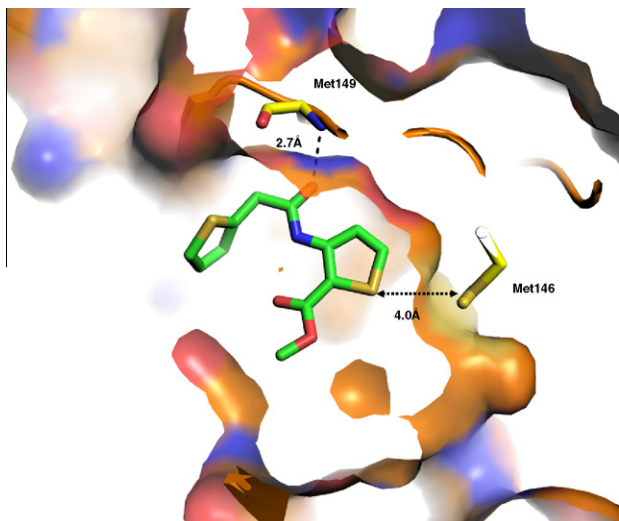Figure 1. In vitro properties for compound 1.[13,16]

Figure 2. Crystal structure of compound **1**, in green, bound to JNK3 in the presence of the JIP1 peptide (2.2 Å resolution). Compound **1** forms a hydrogen bond with Met149 of the hinge while the gatekeeper residue, Met146, lies within proximity to the inhibitor. The PBD deposition code is 3OXI. For experimental conditions see Ref. 15.

The X-ray co-crystal structure of compound **1** is shown in Figure 2. The amide carbonyl of the inhibitor forms a hydrogen bond with the NH of Met149 while the thiophene ring lies within 4 Å of the gatekeeper residue Met146. This crystal structure revealed a large pocket[9] in the vicinity of Met146 and molecular modeling suggested that it would be possible to prepare tri-substituted thiophenes and utilize the third substituent to explore a hydrophobic interaction with the gatekeeper residue Met146.
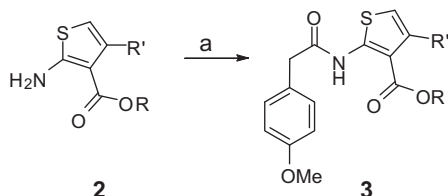
Scheme 1. Reagents and conditions: (a) 4-MeOPhCH$_2$CO$_2$H, POCl$_3$, pyridine, 0 °C, 5 min.

Table 1
SAR of the 4-position of the thiophene

Compd	R'	R	JNK3 IC$_{50}$[a] (µM)	JNK1 IC$_{50}$[a] (µM)	JNK2 IC$_{50}$[a] (µM)
4	Me	Me	0.70	0.59	3.14
5	Et	Me	9.11	19.3	22.5
6	cPr	Et	9.62	15.58	6.29
7	CF$_3$	Et	38.8	18.9	>50
8	CN	Et	0.31	0.35	0.93
9	CCH	Et	3.02	1.05	28.4

[a] Values are means of at least three experiments at 10 µM ATP concentration. See Ref. 13.

Table 2
SAR of the aryl acetamide-4-methyl thiophene

| Compd	R	JNK3 IC$_{50}$[a] (nM)	JNK1 IC$_{50}$[a] (nM)	JNK2 IC$_{50}$[a] (nM)
15		263	283	1838
16		504	597	4524
17		99	295	613
18		226	284	2571
19		1020	686	4150
20		162	95	765
21		110	55	409
22		62	31	863
23		125	78	703

[a] Values are means of at least three experiments at 10 µM ATP concentration. See Ref. 13.
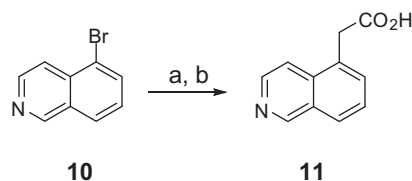
Scheme 2. Reagents and conditions: (a) Pd$_2$(dba)$_3$, Q-Phos, (2-*tert*-butoxy-2-oxoethyl)zinc(II) chloride, THF, rt to 50 °C; (b) HOAc, HCl, reflux.
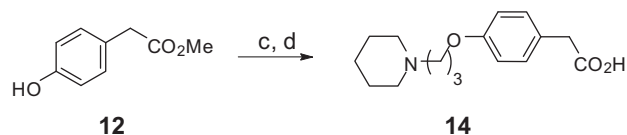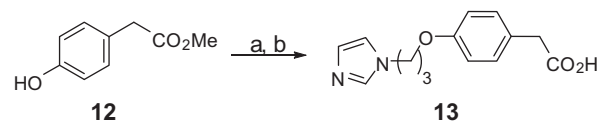
Scheme 3. Reagents and conditions: (a) PPh$_3$, DIAD, 2-(1*H*-imidazol-1-yl)propanol, THF, 70%; (b) HOAc, HCl, reflux; (c) 1-chloro-3-iodopropane, K$_2$CO$_3$, CH$_3$CN, 90 °C; piperidine, NaI, CH$_3$CN, 90 °C; (d) HOAc, HCl, reflux.
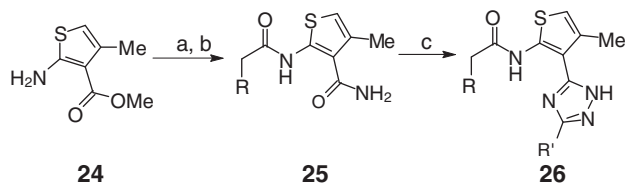
Scheme 4. Reagents and conditions: (a) RCH$_2$CO$_2$H, POCl$_3$, pyridine, 0 °C; (b) NH$_4$Cl, NH$_4$OH (aq); (c) (i) for R' = H dimethylformamide-dimethylacetal, for R' = Me dimethylacetamide-dimethylacetal; (ii) NH$_2$NH$_2$.

A small series of analogs bearing substituents at the 4-position of the thiophene were prepared in order to explore the interaction of the inhibitor with the gatekeeper residue in JNK3. These analogs were readily obtained by POCl$_3$ mediated coupling of the amino thiophenes **2** with 2-(4-methoxyphenyl)acetic acid (Scheme 1) and the JNK inhibition data for these analogs is shown in Table 1. This series of compounds indicated that small substituents such as methyl (**4** JNK3 IC$_{50}$ = 700 nM) and cyano (**8** JNK3 IC$_{50}$ = 310 nM) were well tolerated and gave the expected increase in activity compared to disubstituted thiophenes such as **1**. Larger substituents such as ethyl, cyclopropyl and trifluoromethyl resulted in a dramatic reduction in potency and interestingly, the alkynyl analog **9** lost an order of magnitude of potency compared to nitrile **8**.

Since the 4-methyl thiophene analog **4** gave an improvement in potency, this region of the inhibitor was held constant while the SAR of the acetamide region was explored (Table 2). From our previous report,[8] we demonstrated that replacing the *para*-methoxyphenyl moiety with quinolines, isoquinolines and quinolinones afforded compounds with improved potency. The quinoline, isoquinoline, and quinoxaline analogs were prepared via alpha-arylation of a bromoheterocycle in the presence of Q-phos and Pd$_2$(dba)$_3$[10] as shown in Scheme 2. Phenol analogs were also prepared via a Mitsunobu reaction between phenol **12** and the corresponding alcohol, or by alkylation of phenol **12** with the corresponding halo-alkyls (Scheme 3). After ester hydrolysis the resulting acids were coupled with compound **2** as in Scheme 1 to afford the analogs shown in Table 2.

Replacement of the *para*-methoxyphenyl group with 2-(4-(pyridin-4-yl)phenyl)acetamide gave a three-fold improvement in potency against JNK3 (**15** JNK3 IC$_{50}$ = 263 nM compared to **4** JNK3 IC$_{50}$ = 700 nM) (Table 2). The most potent compound in this series was the 5-isoquinolyl analog **22** (JNK3 IC$_{50}$ = 62 nM), with JNK3

Table 3
SAR of the aryl acetamide

Compd	R	R'	JNK3 IC$_{50}$[a] (nM)	JNK1 IC$_{50}$[a] (nM)	JNK2 IC$_{50}$[a] (nM)	p38α IC$_{50}$[a] (μM)	ERK2 IC$_{50}$[a] (μM)
27	MeO—phenyl—	Me	465	331	824	na	na
28	pyridin-4-yl-phenyl—	Me	324	226	1300	>5	>5
29	piperidine-(CH$_2$)$_3$-O-phenyl—	Me	197	463	1620	>5	>5
30	quinoxalin-5-yl	Me	594	298	230	>5	>5
31	quinolin-5-yl	Me	80	45	81	>50	>50
32	quinolin-5-yl	H	143	105	125	>50	>50
33	3,4-dihydroquinolin-2(1H)-one-5-yl	Me	25	15	42	>50	>50
34	3,4-dihydroquinolin-2(1H)-one-5-yl	H	25	32	31	>50	>50

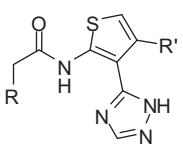[a] Values are means of at least three experiments at 10 μM ATP concentration. See Ref. 13.

Table 4
SAR of the 4-position of the thiophene
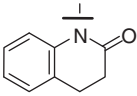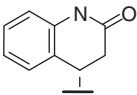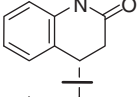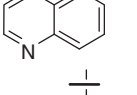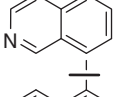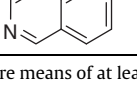
Compd	R	X	JNK3 IC$_{50}$[a] (nM)	JNK1 IC$_{50}$[a] (nM)	JNK2 IC$_{50}$[a] (nM)	p38α IC$_{50}$[a] (μM)	ERK2 IC$_{50}$[a] (μM)
43	3,4-dihydroquinolin-2(1H)-one-5-yl	Br	28	25	42	>20	>50
44	3,4-dihydroquinolin-2(1H)-one-5-yl	Cl	5	4	9	>50	>50
45	3,4-dihydroquinolin-2(1H)-one-5-yl	CN	6	9	8	>50	>50
46	isoquinolin-5-yl	Br	33	28	50	>50	>50
47	isoquinolin-5-yl	Cl	11	14	43	>50	>50
48	isoquinolin-5-yl	CN	7	11	26	>50	>50
49	quinolin-5-yl	Br	34	42	90	>50	>50
50	quinolin-5-yl	Cl	18	15	42	>50	>50
51	quinolin-5-yl	CN	12	12	41	>50	35.1

[a] Values are means of at least three experiments at 10 μM ATP concentration. See Ref. 13.

Table 5
In vitro metabolism, permeability and P-gp efflux data for select compounds

Compd	R	R'	JNK3 IC$_{50}$[a] (nM)	OxMet%[b] (m, h)	P_{app}[b] (nm/s)	P-gp efflux[b]
34	(3,4-dihydroquinolin-2(1H)-one, 4-linked)	Me	25	0, 0	148	3.2
44	(3,4-dihydroquinolin-2(1H)-one, 4-linked)	Cl	5	0, 20	233	0.9
45	(3,4-dihydroquinolin-2(1H)-one, 4-linked)	CN	6	37, 39	180	4.1
32	(quinoline, 5-linked)	Me	143	1, 46	161	1.9
47	(isoquinoline, 5-linked)	Cl	11	29, 50	270	1.6
48	(isoquinoline, 5-linked)	CN	7	48, 62	133	4.6

[a] Values are means of at least three experiments at 10 μM ATP concentration. See Ref. 13.
[b] See Ref. 16.

activity approximately one order of magnitude better than the parent *para*-methoxylphenyl analog **4** (JNK3 IC$_{50}$ = 700 nM).

As we have previously reported,[8,11] it was possible to replace the metabolically labile methyl ester with a heterocycle to obtain compounds which were both more potent and stable than the esters. In particular, it was found that C-linked 1,2,4-triazoles were

amongst the more potent heterocyclic ester replacements and they were therefore combined with the more potent tri-substituted thiophenes. These analogs were prepared as shown in Scheme 4. The commercially available amino thiophene **24** was acylated, the ester converted into a primary amide and finally the primary amide was converted into a 1,2,4-triazole in a two-step procedure involving treatment with DMF–DMA followed by reaction with hydrazine. In this series of analogs the C-methyl triazoles were generally more potent than the monosubstituted triazoles and the biaryl **28** and phenoxy acetamides **27** and **29** proved to be less potent than the fused bicyclic acetamides such as quinoline **31** and dihydroquinolinone **33** (Table 3). All future work focused on the development of these analogs. These triazoles had similar potency for JNK1 compared to JNK3, moderate selectivity over JNK2 and excellent selectivity over the similar kinases p38α and ERK2.

With an optimized left-hand portion of the inhibitor and the triazole as an effective ester replacement the SAR of the 4-position of the thiophene was fine-tuned. It was reasoned that the methyl thiophene would be a metabolic liability (see Table 5 and discussion below) and therefore the methyl group was replaced with small electron withdrawing substituents such as halogens and nitriles. These analogs were prepared as shown in Scheme 5. Thiophene **38** was prepared by reaction of isothiocyanate **35** with ester **36** followed by treatment of the resulting intermediate **37** with POBr$_3$.[12] Aminothiophene **38** was acylated to give **39** which was treated with either copper chloride or copper cyanide followed by elaboration of the methyl ester into the C-linked triazole via primary amide **41** to give the analogs shown in Table 4.

The bromothiophenes were generally less potent against JNK3 compared to the chloro and cyano thiophenes which were essentially equipotent (Table 4). Consistent with previous analogs, the dihydroquinolinones tended to be the more potent analogs with both compounds **44** and **45** displaying single digit nanomolar JNK3 inhibition (JNK3 IC$_{50}$ = 5 and 6 nM, respectively). To our delight no compounds in this series had a measurable IC$_{50}$ against p38α or ERK2 at the concentrations tested. In order to determine the broader kinase selectivity of the thiophene based inhibitors, compound **47** was subjected to a screen of 38 kinases. This screen revealed an exceptionally clean profile with only TTK being inhibited at greater than 50% at 10 μM compound concentration.[14]

The crystal structure of JNK3 in complex with compound **34** in the presence of JIP1 peptide was determined to 2.4 Å resolution as
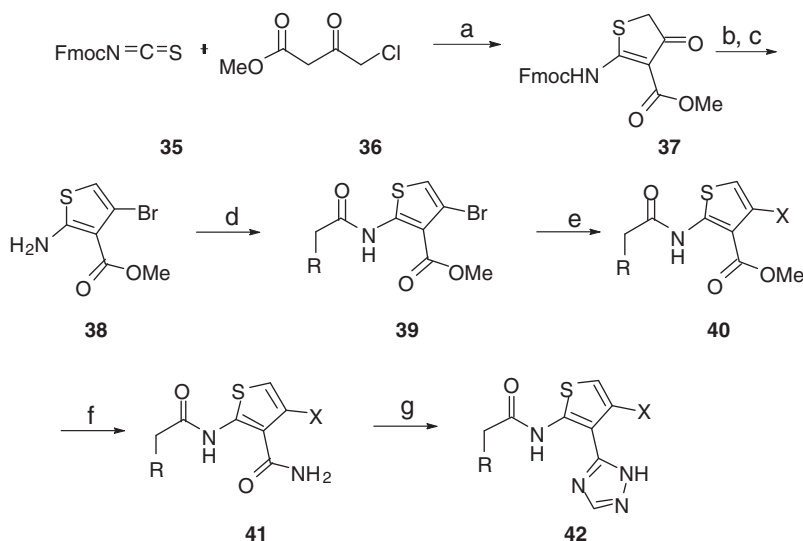
Scheme 5. Reagents and conditions: (a) NaH, hexanes; (b) POBr$_3$, toluene, reflux; (c) morpholine, CH$_2$Cl$_2$, rt; (d) RCH$_2$CO$_2$H, POCl$_3$, pyridine, 0 °C; (e) CuX, DMF, 120 °C; (f) NH$_4$Cl, NH$_4$OH (aq); (g) (i) DMF–DMA; (ii) NH$_2$NH$_2$.
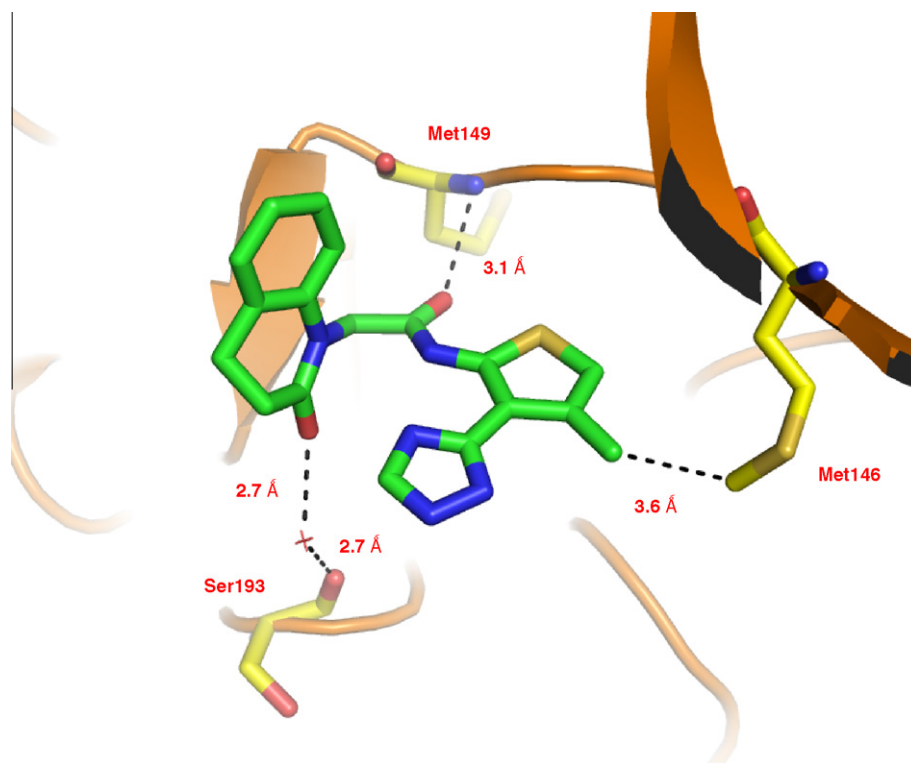
Figure 3. Crystal structure of compound **34** in green bound to JNK3 (2.4 Å resolution). The PBD deposition code is 3PTG. For experimental conditions see Ref. 15.
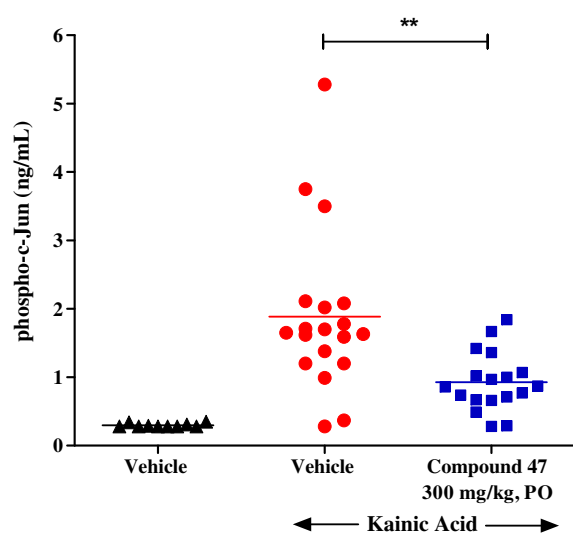

Figure 4. Effect of **47** (300 mg/kg) on phospho-*c*-jun levels in kainic acid (25 mg/kg) treated mice. **p >0.01 significantly different by unpaired *t*-test with Welch correction.

shown in Figure 3. This structure revealed the critical hydrogen bond between the NH of Met149 and the carbonyl of the inhibitor (Fig. 3). The triazole is in plane with the thiophene ring revealing an internal hydrogen bond between the amide NH and the nitrogen of the triazole. The fused bicyclic ring points toward solvent with the carbonyl of the dihydroquinolinone engaged in a hydrogen bond with a water molecule. The methyl at the 4-position of the thiophene lies within proximity to the gatekeeper residue (Met146) and explains why the larger substituents explored in this region were not tolerated (Table 1).

The in vitro metabolism, permeability and P-gp efflux for a selected number of inhibitors are shown in Table 5. As previously mentioned, the 4-methylthiophenes had poor metabolic stability but replacement of the methyl group with a halogen or a nitrile resulted in improved stability. In particular, the combination of the isoquinoline acetamide with the cyanothiophene (**48**) provided the greatest stability. Permeability was generally high for this series of compounds but, unfortunately, the most metabolically stable cyanothiophenes (**45** and **48**) exhibited unacceptable P-gp efflux in MDR-MDCK cells.

Compound **47** exhibited the most favorable combination of potency, metabolic stability, permeability and P-gp efflux and was chosen to be dosed in our kainic acid mouse model. Kainic acid is a potent agonist of a subtype of ionotropic glutamate receptor[17a] and has been shown to induce the activation of MAPK family kinases such as JNK.[17b] The effect of JNK inhibition was tested in kainic acid-treated mice by quantitating the levels of phospho-*c*-jun in brain tissue as a measure of JNK activity. Pretreatment with a single, oral dose of compound **47** at 300 mg/kg resulted in a significant 51% reduction of phospho-*c*-jun in the hippocampus of FVB mice 4 h after an intraperitoneal injection of 25 mg/kg kainic acid (Fig. 4)[18] thus demonstrating the in vivo effect on JNK activity of our inhibitors.

In conclusion, we have expanded the SAR of our thiophene based JNK inhibitors. By optimizing both the arylacetamide region of the inhibitor and the 4-position of the thiophene we obtained single digit nanomolar compounds which, when dosed orally, demonstrated a robust in vivo effect on JNK activity as measured by phospho-*c*-jun reduction in our kainic acid mouse model. Further optimization of these inhibitors to improve their pharmacokinetic properties will be reported in due course.

Acknowledgments

Supplementary data

Supplementary data associated with this article can be found, in the online version, at doi:10.1016/j.bmcl.2011.01.046.

References and notes

1. (a) Siddiqui, M. S.; Reddy, P. A. *J. Med. Chem.* **2010**, *53*, 3005; (b) Bogoyevitch, M. A.; Ngoei, K. R. W.; Zhao, T. T.; Yeap, Y. Y. C.; Ng, D. C. H. *Biochim. Biophys. Acta* **2010**, *1804*, 463; (c) Haeusgen, W.; Boehm, R.; Zhao, Y.; Herdegen, T.; Waetzig, V. *Neuroscience* **2009**, *161*, 951; (d) LoGrasso, P.; Kamenecka, T. *Mini-Rev. Med. Chem.* **2008**, *8*, 755; (e) Bogoyevitch, M. A.; Arthur, P. G. *Biochim. Biophys. Acta* **2008**, *1784*, 76; (f) Bogoyevitch, M. A.; Kobe, B. *Microbiol. Mol. Biol. Rev.* **2006**, *70*, 1061; (g) Kim, W. H.; Lee, J. W.; Gao, B.; Jung, M. H. *Cell. Signal.* **2005**, *17*, 1516; (h) Han, S.-Y. *Toxicol. Res.* **2008**, *24*, 93.
2. (a) Derijard, B.; Hibi, M.; Wu, I. H.; Barrett, T.; Su, B.; Deng, T.; Karin, M.; Davis, R. J. *Cell* **1994**, *76*, 1025; (b) Luo, Y.; Umegaki, H.; Wang, X.; Abe, R.; G.S. *J. Biol. Chem.* **1998**, *273*, 3756; (c) Kerkela, R.; Grazette, L.; Yacobi, R.; Iliescu, C.; Patten, R.; Beahm, C.; Walters, B.; Shevtson, S.; Pesant, S.; Clubb, F. J.; Rosenzweig, A.; Salomon, R. N.; Van Etten, R. A.; Alroy, J.; Durand, J. B.; Force, T. *Nat. Med.* **2006**, *12*, 908; (d) Nishitoh, H.; Matsuzamu, A.; Tobiume, K.; Saegusa, K.; Takeda, K.; Inoue, K.; Hori, S.; Kaakizuka, A.; Ichijo, H. *Genes Dev.* **2002**, *16*, 1345; (e) Urano, F.; Wang, X.; Bertolottie, A.; Zhang, Y.; Chung, P.; Harding, H. P.; Ron, D. *Science* **2000**, *287*, 664; (f) LoGrasso, P.; Kamenecka, T. *Mini-Rev. Med. Chem.* **2008**, *8*, 755. and references herein.
3. (a) Kallunki, T.; Su, B.; Tsigelny, I.; Sluss, H. K.; Derijard, B.; Moore, G.; Davis, R.; Karin, M. *Genes Dev.* **1994**, *8*, 2996; (b) Sluss, H. K.; Barrett, T.; Derijard, B.; Davis, R. *J. Mol. Cell Biol.* **1994**, *14*, 8376; (c) Mohit, A. A.; Martin, J. H.; Miller, C. A. *Neuron* **1995**, *14*, 67.
4. Chang, L.; Jones, Y.; Ellisman, M. H.; Goldstein, L. S.; Karin, M. *Dev. Cell* **2003**, *4*, 521.
5. (a) Borsello, T.; Forloni, G. *Curr. Pharm. Des.* **2007**, *13*, 1875; (b) Wang, W.; Ma, C.; Mao, Z.; Li, M. *Drug News Perspect.* **2004**, *17*, 646; (c) Resnick, L.; Fennell, M. *Drug Discovery Today* **2004**, *9*, 932; (d) Harper, S. J.; Wilkie, N. *Expert Opin. Ther. Targets.* **2003**, *7*, 187; (e) Manning, A. M.; Davis, R. J. *Nat. Rev. Drug Disc.* **2003**, *2*, 554.
6. (a) Yang, D. D.; Kuan, C. Y.; Whitmarsh, A. J., et al *Nature* **1997**, *389*, 865; (b) Kuan, C. Y.; Whitmarsh, A. J.; Yang, D. D.; Liao, G.; Schloemer, A. J.; Dong, C.; Bao, J.; Banasiak, K. J.; Haddad, G. G.; Flavell, R. A.; Davis, R. J.; Rakic, P. *Proc. Natl. Acad. Sci. U.S.A. 100*, 15184.
7. (a) Christopher, J. A.; Atkinson, F. L.; Bax, B. D.; Brown, M. J. B.; Champigny, A. C.; Chuang, T. T.; Jones, E. J.; Mosley, J. E.; Musgrave, J. R *Bioorg. Med. Chem. Lett.* **2009**, *19*, 2230; (b) Angell, R. M.; Atkinson, F. L.; Brown, M. J.; Chuang, T. T.; Christopher, J. A.; Cichy-Knight, M.; Dunn, A. K.; Hightower, K. E.; Malkakorpi, S.; Musgrave, J. R.; Neu, M.; Rowland, P.; Shea, R. L.; Smith, J. L.; Somers, D. O.; Thomas, S. A.; Thompson, G.; Wang, R. *Bioorg. Med. Chem. Lett.* **2007**, *17*, 1296; (c) Swahn, B.-M.; Xue, Y.; Arzel, E.; Kallin, E.; Magnus, A.; Plobeck, N.; Viklund, J. *Bioorg. Med. Chem. Lett.* **2006**, *16*, 1397; (d) Swahn, B.-M.; Huerta, F.; Kallin, E.; Malmström, J.; Weigelt, T.; Viklund, J.; Womack, P.; Xue, Y.; Öhberg, L. *Bioorg. Med. Chem. Lett.* **2005**, *15*, 5095.
8. Hom, R. K.; Bowers, S.; Sealy, J. M.; Truong, A. P.; Probst, G. D.; Neitzel, M. L.; Neitz, R. J.; Fang, L.; Brogley, L.; Wu, J.; Konradi, A. W.; Sham, H. L.; Tóth, G.; Pan, H.; Yao, N.; Artis, D. R.; Quinn, K.; Sauer, J.-M.; Powell, K.; Ren, Z.; Bard, F.; Yednock, T.; Griswold-Prenner, I. *Bioorg. Med. Chem. Lett.* **2010**, *20*, 7303.
9. Scapin, G.; Patel, S. B.; Lisnock, J.; Becker, J. W.; LoGrasso, P. V. *Chem. Biol.* **2003**, *10*, 705.
10. Hama, T.; Culkin, D. A.; Hartwig, J. F. *J. Am. Chem. Soc.* **2006**, *128*, 4976.
11. Sham, H. L.; Konradi, A. W.; Hom, R. K.; Probst, G. D.; Bowers, S.; Truong, A.; Neitz, R. J.; Sealy, J.; Toth, G. WO2010091310, 2010.
12. Faull, A. W.; Hull, R. *J. Chem. Soc., Perkin Trans. 1* **1981**, *4*, 1078.
13. Details on the TR-FRET enzyme assays can be found in the Supplementary data.
14. Full kinase panel data performed at Invitrogen are included in Supplementary data.
15. Details on the crystallization conditions are included in the Supplementary data.
16. For conditions of in vitro pharmacokinetic assays, see: Truong, A. P.; Aubele, D. A.; Probst, G. D.; Neitzel, M. L.; Semko, C. M.; Bowers, S.; Dressen, D.; Hom, R. K.; Konradi, A. W.; Sham, H. L.; Garofalo, A. W.; Keim, P. S.; Wu, J.; Dappen, M. S.; Wong, K.; Goldbach, E.; Quinn, K. P.; Sauer, J.-M.; Brigham, E. F.; Wallace, W.; Nguyen, L.; Hemphill, S. S.; Bova, M. P.; Basi, G. *Bioorg. Med. Chem. Lett.* **2009**, *19*, 4920.
17. (a) Jeon, S. H.; Kim, Y.-S.; Bae, C.-D.; Park, J.-B. *Exp. Mol. Med.* **2000**, *32*, 227; (b) Kim, Y.-H.; Choi, S.-S.; Lee, J.-K.; Won, J.-S.; Choi, M.-R.; Suh, H.-W. *Mol. Cells* **2001**, *11*, 144.
18. Details on the study of compound **47** in our kainic acid mouse model can be found in the Supplementary data.